Polyhedron 152 (2018) 22–30

Contents lists available at ScienceDirect

Polyhedron

journal homepage: www.elsevier.com/locate/poly

Structural characterization, hydrolytic stability and dynamics of *cis*-$Mo^{VI}O_2^{2+}$ hydroquinonate/phenolate complexes

Chryssoula Drouza [a,*], Sofia Hadjithoma [b], Maria Nicolaou [b], Anastasios D. Keramidas [b,*]

[a] Department of Agricultural Sciences, Biotechnology and Food Science, Cyprus University of Technology, Lemesos 3036, Cyprus
[b] Department of Chemistry, University of Cyprus, 2109 Nicosia, Cyprus

ARTICLE INFO

Article history:
Received 30 March 2018
Accepted 1 June 2018
Available online 15 June 2018

Dedicated to Professor Spyros Perlepes on the Occasion of His 65th Birthday.

Keywords:
Molybdenum
Hydroquinones
Non-innocent ligands
Kinetics
Hydrolytic stability

ABSTRACT

Although, the investigation of the interactions of Mo^{VI} ion with the "non-innocent" phenols/hydroquinones is essential for the understanding of the role of molybdenum in the biological systems, the Mo^{VI} complexes of phenolate/hydroquinonate and their functionalized variants remain mainly unexplored. Reaction of $Na_2Mo^{VI}O_4$ with tripod iminodiacetate phenol/hydroquinone ligands in aqueous solutions resulted in the synthesis of mononuclear phenolate/hydroquinonate and dinuclear bridged-hydroquinonate *cis*-$Mo^{VI}O_2^{2+}$ complexes. The new complexes were isolated and characterized in solid state by X-ray crystallography. The ^1H, ^{13}C and ^{95}Mo NMR spectra of the aqueous solutions of the complexes show that they retain their structure at the pD range 2–4, with the dinuclear bridged-hydroquinonate *cis*-$Mo^{VI}O_2^{2+}$ to form two isomers which are in dynamic equilibrium. At pDs 4–7 the Mo^{VI}-$O_{phenolate}$ bond of the *cis*-$Mo^{VI}O_2^{2+}$ compounds hydrolyzes to form $Mo^{VI}O_3$-iminodiacetate species. Variable temperature (VT) and 2D {^1H} EXSY NMR spectroscopies where employed for the determination of the thermodynamic and activation parameters of the isomerization reaction between the dinuclear bridged-hydroquinonate *cis*-$Mo^{VI}O_2^{2+}$ isomers. The exchange mechanism between *cis*-$Mo^{VI}O_2^{2+}$ and the $Mo^{VI}O_3$ species were also investigated by 2D {^1H} EXSY NMR spectroscopy. Despite of the higher strength of the Mo^{VI}-$O_{phenolate}$ bond, it is more labile than the Mo^{VI}-$O_{carboxylate}$ bond. The rate determining step of the above exchange reactions was found to be the dissociation of the phenolate/hydroquinonate oxygen atom from Mo^{VI} ion.

1. Introduction

Molybdenum ion has been found to be an important biological element participating in several enzymatic reactions whereas administration of molybdate to biological organisms induces biological response [1–4], including antidiabetic and anticancer activity [5–9]. Mimicking the active center of the molybdenum enzymes, several molybdenum complexes have been synthesized, exhibiting oxygen transfer, N_2 and C–H activation and epoxidation catalytic properties [2,10–18].

The interactions of molybdenum enzymes with phenols and dioxolenes in biological systems are important either for the molybdenum redox recycling or for the catalytic activity of proteins [16,17,19,20]. The oxidative power of Mo^{VI} has been used also for the determination of phenol contents in foods [21–23]. A popular and fast method is the Folin–Ciocalteu method which is based on the development of a blue color of the Mo^{V} ions after the oxidation of phenol compounds in alkaline solution with a molybdotungstophosphate heteropolyanion reagent ($3H_2O$-P_2O_5-$13W^{VI}O_3$-$5Mo^{VI}O_3$-$10H_2O$). An emerging technology is the development of new ligands for the selective separation of Mo^{VI} from other metal ions, such as V^{V} and W^{VI}, targeting the recycling of molybdenum and its removal from the environment [24–27]. On the other hand, hydroquinones are important proton/electron sources and sinks that play an essential role in electron/proton coupled biochemical processes [28–32]. Covalently bonded molecules of strong oxidizing metal ions with "non-innocent" ligands [33], such as hydroquinones, have provided unique well-defined model systems to probe the mechanisms of either thermal or proton induced electron transfer reactions [34–38].

Despite of the importance of the interaction of the Mo^{VI} ion with the hydroquinones in biological systems, only one example of a structurally characterized Mo^{VI}-hydroquinone complex has been reported up to now [39]. This is mainly due to the reduction of Mo^{VI} from hydroquinones to Mo^{V} and the absence of a chelate coordination site in a simple hydroquinone. A strategy to prepare such species is to synthesize substituted p-hydroquinones in *o*-position with substituents containing hard donor atoms, thus, enabling the metal atom to form chelate rings.

* Corresponding authors. Fax: +357 22895454.
E-mail addresses: chryssoula.drouza@cut.ac.cy (C. Drouza), akeramid@ucy.ac.cy (A.D. Keramidas).

https://doi.org/10.1016/j.poly.2018.06.008
0277-5387/

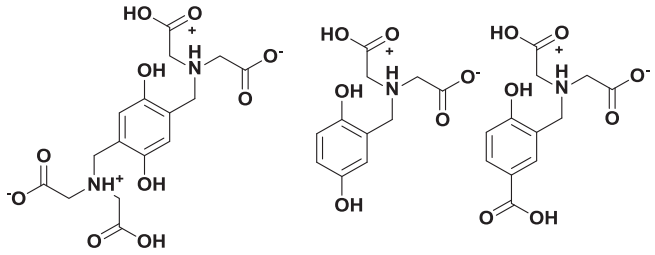

Scheme 1. Drawings of the ligands in this study.

Here in, we present the structural and aqueous solution properties of Mo^{VI} complexes with phenolate/hydroquinonate ligands substituted with iminodiacetic group at *o*-position (Scheme 1). The iminodiacetate substituents have been employed in order to stabilize molybdenum in oxidation state VI [40], concurrently with the stabilization of the hydroquinone ligation to the metal ion. In addition, coordination of the metal ion to the negative charged carboxylate groups results in water soluble negative charged complexes, permitting the exploration of molybdate-phenolate chemistry in aqueous solution, thus, simulating better the biological media. The syntheses of the bridging ligand H_6cahq and its $(cis\text{-}Mo^{VI}O_2^{2+})_2$ dinuclear complex have been motivated by the improved catalytic and photocatalytic properties of the bridged dinuclear versus the mononuclear complexes [36,41,42]. The $cis\text{-}Mo^{VI}O_2^{2+}$ – $cahq^{-6}$ complex is the first dinuclear bridged σ-bonded hydroquinonate complex of Mo^{VI} reported in the literature. These Mo^{VI} complexes are hydrolytically stable in acidic pHs exhibiting an intramolecular exchange through opening of the phenolate/hydroquinonate chelate ring.

2. Experimental

Reagent grade $Na_2Mo^{VI}O_4$, hydroquinone and iminodiacetic acid were purchased from Aldrich. All chemicals were used without further purification. UV spectra were recorded on a Shimadzu UV-1601 Spectrophotometer. The ligands referred to this study, 2,5-bis[N,N′-bis(carboxymethyl)aminomethyl]-hydroquinone (H_6cahq), 2-[N,N′-bis(carboxymethyl)aminomethyl]-hydroquinone (H_3mcah) and 2-[N,N′-bis(carboxymethyl)aminomethyl]-1,4-hydrobenzoic (H_3capc), were synthesized based on the Mannich type reaction reported in the literature [34,43,44].

2.1. Synthesis of $Na_2[(MoO_2)_2(\mu\text{-cahq})]\cdot 3.5H_2O$ (**1**)

A solution prepared by dissolving $Na_2MoO_4\cdot 2H_2O$ (1.20 g, 4.95 mmol) in 3 mL H_2O was added to a in 5 mL H_2O suspension of H_6cahq (1.00 g. 2.36 mmol). The pH of the resulting deep red solution was adjusted at 3.5 using an aqueous solution of HCl (6 N). The solution was filtered and kept at 4 °C for 24 h. The deep red precipitation was filtered under vacuum. The solid was recrystallized with H_2O. The yield was 1.47 g (82%). Single crystals for X-ray analysis were obtained by slow diffusion of CH_3OH in a concentrated aqueous solution of complex **1**. Elemental Analysis for $C_{16}H_{14}N_2O_{14}Mo_2Na_2\cdot 3.5H_2O$; Calc.: C, 25.31; H, 2.79; N, 3.69; Found: C, 25.25; H, 2.81; N, 3.68%.

2.2. Synthesis of $K[(MoO_2)mcah]\cdot H_2O$ (**2**)

H_3mcah (1.00 g, 3.92 mmol) dissolved in 10 mL H_2O with the dropwise addition of KOH (5 N). $Na_2MoO_4\cdot 2H_2O$ (0.94 g, 3.9 mmol) dissolved in 5 mL H_2O was added in the above solution and the pH of the solution was adjusted at 4.3 with 6 N HCl. The deep red solution was kept at 4 °C for 3 days resulting in the precipitation of a red crystals suitable for X-ray analysis. The crystals were filtered, washed with ethanol and dried under vacuum. The yield was 1.77 g (89%). Elemental Analysis for $C_{11}H_{10}KMoNO_8.H_2O$; Calc.: C, 30.21; H, 2.77; N, 3.20; Found: C, 30.40; H, 2.61; N, 3.27%.

2.3. Synthesis of $Na[(MoO_2)capc]\cdot H_2O$ (**3**)

The pH of a suspension of H_3capc (0.60 g, 2.3 mmol) in 5 mL H_2O was adjusted at 5.0 with the addition of aqueous NaOH (5 M). Then, $Na_2MoO_4.2H_2O$ (1.45 g, 4.75 mmol) was added to the above solution, and the pH was adjusted at 4.0 with aqueous HCl (4 N). The yellow solution was kept at 4 °C for 24 h resulting in the precipitation of a yellow solid. The precipitate was filtered under vacuum and recrystallized with H_2O. The yield was 0.75 g (73 %). Single crystals for X-ray analysis were obtained by slow diffusion of CH_3OH in a concentrated aqueous solution of complex **3**. Elemental Analysis for $C_{12}H_{10}NO_{10}MoNa\cdot H_2O$; Calc.: C, 30.98; H, 2.60; N, 3.01; Found: C: 30.16, H:2.57, N: 3.10%.

2.4. X-ray crystallography

Intensity data for all compounds were measured on a XCalibur III 4-cycle diffractometer, equipped with a CCD camera detector, using a monochromated Mo Kα ($\lambda = 0.71073$ Å) radiation at 100 K. In all cases, analytical absorption corrections were applied. The structures were solved by direct methods using the program SHELX-97 [45,46] and refined on F^2 by a full-matrix least-squares procedure with anisotropic displacement parameters for all the non-hydrogen atoms based on all data minimizing $wR = [\Sigma w(|F_o|^2 - |F_c|^2)/\Sigma w|F_o|^2]^{1/2}$, $R = \Sigma||F_o| - |F_c||/\Sigma|F_o|$, and $GOF = [\Sigma[w(F_o^2 - F_c^2)^2]/(n-p)]^{1/2}$, $w = 1/[\sigma^2(F_o^2) + (aP)^2 + bP]$, where $P = (F_o^2 + 2F_c^2)/3$ [45,46]. A summary of the relevant crystallographic data and the final refinement details is given in Table S1. The positions of hydrogen atoms were calculated from stereochemical considerations and kept fixed isotropic during refinement or found in the D*F* map and refined with isotropic thermal parameters.

2.5. NMR spectroscopy

NMR spectra were recorded on a Bruker Avance 300 at 300.13, 75.476 and 13.029 MHz for ^1H, ^{13}C, and ^{95}Mo NMR respectively. The 1D ^1H and ^{13}C NMR spectra were acquired with a 30° pulse width and a 2.0 s delay time (in D_2O solvent). The 1D ^{95}Mo NMR spectra were acquired with a 90° pulse width and a 0.1 s delay time (in D_2O solvent). All experiments were done in duplicate.

T_1 measurements were obtained by using the inversion recovery method. The phase sensitive 2D ^1H COSY-45 experiments (pulse sequence 90°-t_1-45°) were measured using 256 increments (each consisting of 16 scans) covering the full spectrum (10 ppm in both dimensions). The standard NOESY pulse sequence (90°-t_1-90°-t_m-90°) was used in the 2D ^1H EXSY-NOESY measurements. These spectra were acquired using 512 increments of 1 K size (64 scans each) covering full spectrum (10 ppm in both dimensions) or partial (3–4 ppm) regions of the spectrum. The delay time used in the 2D spectra was 3.0 s, based on the measured T_1 values. Variable mixing times ranging from 0 to 1.00 s were used. All NMR samples were prepared by dissolving the crystalline compounds in D_2O at room temperature.

The variable temperature NMR experiments (VT) require that the NMR spectrometer be calibrated to each temperature value within ±1 °C, using a 4% CH_3OH/CD_3OD sample for the low temperature region, and 80% ethylene glycol/d_6-DMSO sample for the high